JOC The Journal of Organic Chemistry

Article

pubs.acs.org/joc

Amorphous Solid Simulation and Trial Fabrication of the Organic Field-Effect Transistor of Tetrathienonaphthalenes Prepared by Using Microflow Photochemical Reactions: A Theoretical Calculation-Inspired Investigation

Atsushi Yamamoto,[†] Yasunori Matsui,[†] Toshio Asada,[‡] Motoki Kumeda,[†] Kenichiro Takagi,[§] Yu Suenaga,[§] Kunihiko Nagae,[†] Eisuke Ohta,[†] Hiroyasu Sato,[∥] Shiro Koseki,[‡] Hiroyoshi Naito,[§] and Hiroshi Ikeda*[,†]

[†]Department of Applied Chemistry, Graduate School of Engineering, [‡]Department of Chemistry, Graduate School of Science, [§]Department of Physics and Electronics, Graduate School of Engineering, Osaka Prefecture University, 1-1 Gakuen-cho, Naka-ku, Sakai, Osaka 599-8531, Japan

[∥]Rigaku Corporation, 3-9-12 Matsubara-cho, Akishima, Tokyo 196-8666, Japan

Supporting Information

ABSTRACT: The p-type organic semiconductor (OSC) material tetrathieno[2,3-*a*:3′,2′-*c*:2″,3″-*f*:3‴,2‴-*h*]naphthalene (2TTN) and its alkyl-substituted derivatives C_n-2TTNs (n = 6, 8, and 10) have been developed based on the results of theoretical calculation-inspired investigation. A hole mobility for amorphous C_n-2TTNs (10^{-2}–10^{-3} cm^2 V^{-1} s^{-1}) was accurately predicted by using a novel statistical method in which the geometric mean of the mobilities for many individual small molecular flocks in an amorphous solid was obtained by using molecular mechanical molecular dynamics simulations and quantum chemical calculations. The simulation also suggests that upon increasing the length of alkyl chains in C_n-2TTNs the mobilities become smaller as a consequence of a decrease in transfer integral values. C_n-2TTNs are synthesized in a microflow reactor through photoreactions of the corresponding precursors. C_n-2TTNs are then utilized in the fabrication of organic field-effect transistors (OFETs). Although spin-coated thin films of C_n-2TTNs are crystalline, the hole mobilities (10^{-2}–10^{-3} cm^2 V^{-1} s^{-1}) of trial OFETs decrease upon elongation of the alkyl chains. This finding parallels the results of theoretical simulation. The simulation method for amorphous solids developed in this effort should become a useful tool in studies aimed at designing new OSC materials.

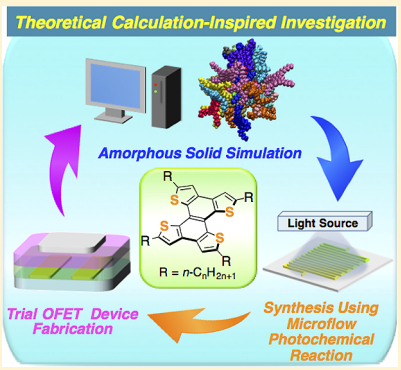

INTRODUCTION

Organic semiconductors (OSCs) are employed in various electronic applications including organic light-emitting diodes,[1] organic photovoltaic cells,[2] and organic field-effect transistors (OFETs).[3] In the past two decades, many polycyclic aromatic compounds have been developed as high-performance OSC materials.[4] In addition, the results of several studies show that the performance of these materials is controlled by solid-state molecular orientation governed by intermolecular interactions (e.g., π–π, CH–π, and S–S interactions). Actually, some one-dimensional π-electronic systems[5] exhibit high charge carrier mobilities as a result of their close-packed crystalline structures. For example, dinaphtho[2,3-*b*:2′,3′-f]thieno[3,2-*b*]thiophene (DNTT)[5f] and 2,7-diphenyl[1]benzothieno[3,2-*b*][1]-benzothiophene (DPh-BTBT)[5h] are known to be high-performance OSC materials (Chart 1). Recently, a number of new OSC materials possessing two-dimensional π-electronic systems[6] have been described. These materials show high mobilities owing to the existence of extensive intermolecular π–π overlap in the solid state.[7] However, the solubilities of these two-dimensional materials in organic solvents are low, and as a result, it is difficult to prepare them in thin film forms by using solution processes. Therefore, it is necessary to introduce conformationally flexible substituents[8] such as long alkyl chains to overcome the solubility problem.

Chart 1. Molecular Structures of DNTT, DPh-BTBT, and 3TTN

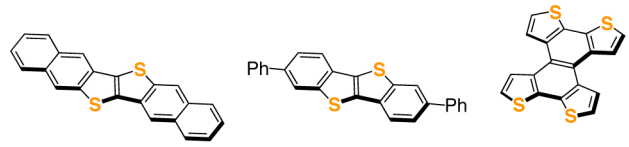

Methods involving photoinduced 6π-electrocyclization followed by dehydrogenation have been employed to prepare cyclic, extensively conjugated π-electron systems.[9] By using this

Received: January 18, 2016
Published: March 24, 2016

DOI: 10.1021/acs.joc.6b00117
J. Org. Chem. 2016, 81, 3168–3176

approach, we previously prepared tetrathieno[3,2-*a*:2′,3′-*c*:3″,2″-*f*:2‴,3‴-h]naphthalene (3TTN) from tetra(thien-3-yl)-ethane.[10] The results of this effort led to the conclusion that 3TTN meets two requirements for serving as a p-type OSC material, including high stability against molecular oxygen and a columnar crystal-packing structure that enables efficient intermolecular $\pi-\pi$ interactions. In this connection, tetrathieno[2,3-*a*:3′,2′-*c*:2″,3″-*f*:3‴,2‴-*h*]naphthalene (2TTN, Scheme 1),[11] a structural isomer of 3TTN, is also an attractive

Scheme 1. Formations of 2TTN and C_n-2TTNs by Using Sequential Photoinduced 6π-Electrocyclization–Dehydrogenation Reactions

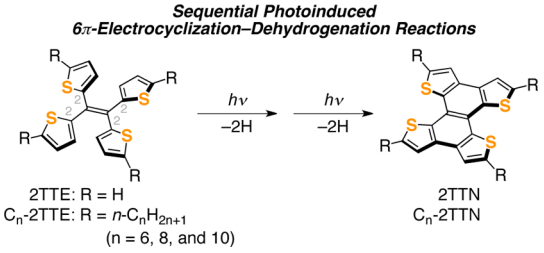

candidate as OSC materials. However, no reports exist describing the properties of the parent 2TTN as an OSC material. In contrast, the involvement of 2TTN in formation of charge-transfer complexes with 7,7,8,8-tetracyanoquinodimethane[11] and a determination of high electron-donating ability of its derivatives[12a,b] leading to a unique crystal packing structure[12c] have been reported.

Below, we describe the results of an investigation in which several features of 2TTN and C_n-2TTNs (n = 6, 8, and 10) were explored. First, theoretical simulations of the amorphous solid structures along with the application of a novel statistical method provided insight into the hole mobilities of these compounds. Next, an efficient method for the synthesis of C_n-2TTNs, using microflow photochemical reactions, was developed.[13] Finally, C_n-2TTNs were employed in the fabrication of OFET devices. The hole mobilities of trial top-gate bottom-contact OFET devices were found to correlate well with the results of theoretical mobilities.

RESULTS AND DISCUSSION

Hole-Transporting Simulation of 2TTN and C_n-2TTNs in Amorphous Solid Structures. The availability of an accurate theoretical method to investigate OSC characteristics in the amorphous solid structure would accelerate the development of OSC materials. Driven by this goal, we devised a method to estimate the hole mobility (μ_{am}) of 2TTN and C_n-2TTNs in an amorphous solid structure (Figure 1) using molecular mechanical molecular dynamics (MM-MD) simulations[14] and quantum-chemical calculations[15] (HF/6-31G). The simulated amorphous solid structures of these compounds were determined in the following manner. The initial ordered configuration of 480 (= 6 × 5 × 16) molecules of 2TTN and C_n-2TTNs in a unit cell was generated by using the leap module of the AMBER 9 package,[16] in which MM force fields of the molecules are generated by using the antechamber module. An MM-MD simulation was performed for 2 ns at a temperature of 1000 K to generate random configurations under periodic boundary conditions. The time step in this simulation was taken as 1 fs. Then, the system was gradually cooled to 300 K for a

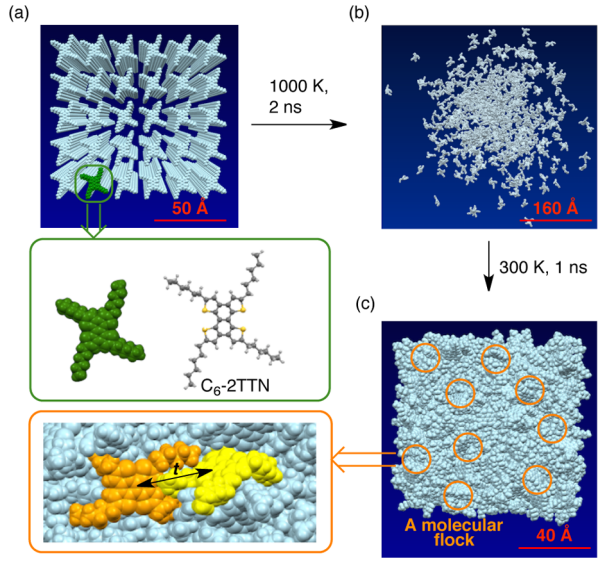

Figure 1. Method for preparation of the simulated amorphous solid structure of C_6-2TTN: (a) initial ordered configuration, (b) random configuration, and (c) amorphous solid structure. The transfer integral (t) between adjacent molecules in molecular flocks (orange circles).

period of 1 ns. The density (D) of the constructed amorphous solid structure was calculated to be ca. 1.0–1.5 g cm^{-3} (Table 1), which is reasonable for an organic material.

Table 1. Densities (D), Hole Mobilities (μ_{am}), and Transfer Integrals (t) between Adjacent Molecules of 2TTN and C_n-2TTNs in Simulated Amorphous Solid Structures

compd	D (g cm^{-3})	μ_{am}[a] (cm^2 V^{-1} s^{-1})	t[b,c] (meV)
2TTN	1.49	4.6×10^{-2}	30.7
C_6-2TTN	1.06	2.1×10^{-2}	20.2
C_8-2TTN	1.01	9.3×10^{-3}	18.7
C_{10}-2TTN	0.99	1.8×10^{-3}	12.9

[a]Obtained as the geometric mean. [b]Calculated by using HF/6-31G. [c]Obtained as the arithmetic mean.

From a microscopic viewpoint, hole transport in the thin film of 2TTN (or C_n-2TTNs) involves continuous single-electron transfer (SET) from 2TTN (or C_n-2TTNs) to 2TTN$^{\bullet+}$ (or C_n-2TTNs$^{\bullet+}$). For molecular flocks consisting of a given focused molecule and ca. 30 surrounding partner molecules within a 5 Å radius, the rate constant (W) for SET in each molecular pair can be described by using the Marcus equation (eq 1)[17]

$$W = \frac{2\pi t^2}{h}\left(\frac{\pi}{\lambda_{RE} k_B T}\right)^{1/2} \exp\left[-\frac{(\Delta G + \lambda_{RE})^2}{4\lambda_{RE} k_B T}\right] \quad (1)$$

where t is a transfer integral[18,19] for the molecular pair, h is Planck's constant, λ_{RE} is reorganization energy,[20] k_B is the Boltzmann constant, T is the temperature, and ΔG is the Gibbs free energy change associated with SET. To conserve computational costs, the amorphous solid structures were regarded as being homogeneous. As a result, ΔG associated with hole transfer is 0. Furthermore, μ_{am} is taken to be the geometric mean of the modified Stokes–Einstein equation (eq 2)[21]

$$\mu_{am} = \prod_N \left(\frac{1}{6}\frac{e}{k_B T}\frac{\sum_i r_i^2 W_i^2}{\sum_j W_j}\right)^{1/N} \quad (2)$$

DOI: 10.1021/acs.joc.6b00117
J. Org. Chem. 2016, 81, 3168–3176

where N is the number of molecular flocks, e is the elementary charge, and r is the distance between molecular centroids. The local structure in the amorphous solid phase is rather rigid and disordered at room temperature. The transfer integrals are dominantly affected not only by overlap integrals but also by the relative configurations for two molecules. Therefore, the hole mobility evaluated with calculated transfer integrals between two molecules are reluctant to converge when the simple averaging technique within a very limited pair of molecules is used. Note that μ_{am} values for several OSC materials, estimated by using the geometric mean, were recently found[22] to correlate well with experimentally determined hole mobilities. Using this approach, we found that μ_{am} values are calculated to be 4.6×10^{-2}, 2.1×10^{-2}, 9.3×10^{-3}, and 1.8×10^{-3} cm^2 V^{-1} s^{-1} for 2TTN, C_6-, C_8-, and C_{10}-2TTNs, respectively. The values tend to decrease as the length of the alkyl chain in these substances increases as a consequence of a reduction of t. The results suggest that among C_n-2TTNs, the one with shortest C_6 alkyl chain (C_6-2TTN) has the highest mobility and, thus, is the best candidate for an OSC material.

Syntheses of the 2TTN and C_n-2TTNs. A general method was devised for synthesis of 2TTN and C_n-2TTNs (Scheme 2).

Scheme 2. Syntheses of 2TTE and C_n-2TTEs

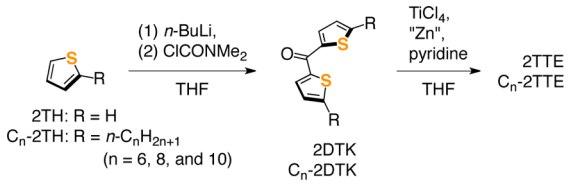

The precursors tetra(thien-2-yl)ethene (2TTE) and C_n-2TTEs were prepared from di(thien-2-yl) ketone (2DTK) and C_n-2DTKs, respectively, by using McMurry coupling reactions.[11,23] Photoirradiation of a solution of 2TTE and I_2 in C_6H_6 for 15 h, using a batch reactor with a 300 W high-pressure mercury lamp through a Pyrex cutoff filter ($\lambda_{EX} \geq 313$ nm), gives rise to formation of 2TTN in a 35% yield (Table 2, entry 1). Alternatively, 2TTN is produced in a 56% yield when a solution of 2TTE in CH_2Cl_2 containing p-chloranil (p-CA)[9b,c] serving as an electron acceptor is subjected to the same photoreaction conditions (entry 2). Photoreaction of C_6-2TTE in CH_2Cl_2 containing p-CA, using a microflow reactor[22] equipped with a 300 mW UV–LED lamp (λ_{EX} = 365 nm) through a quartz glass, generates C_6-2TTN in a 60% yield (entry 3). In contrast, a similar reaction using a batch reactor also formed C_6-2TTN but in only a 40% yield (entry 4). In addition, photoreactions (80 W medium-pressure mercury lamp through a Pyrex cutoff filter, $\lambda_{EX} \geq 313$ nm) of C_8- and C_{10}-2TTE in CH_2Cl_2 solutions containing p-CA using the microflow reactor also produce C_8- and C_{10}-2TTNs in 73% and 36% yields, respectively. The results show that these photoreactions take place more efficiently when a microflow rather than a traditional batch reactor is employed (entries 5–8).

Physical Properties of 3TTN, 2TTN, and C_n-2TTNs. The physical properties of TTNs were assessed to gain insight into their possible use as OSC materials. Differential scanning calorimetry (DSC) measurements[22] were utilized to elucidate their thermal properties. The results show that 2TTN does not undergo phase transition in the range of 40 to 350 °C, suggesting that this substance has high thermal stability. This observation contrasts with that obtained from studies of 3TTN, which show that a small endothermic peak occurs in the scan at ca. 280 °C (solid–solid phase transition) and a large exothermic peak exists at ca. 330 °C (thermal decomposition). DSC traces of C_n-2TTNs are shown as endothermic peaks at ca. 100 and 115 °C (both solid–liquid phase transitions) and exothermic peaks at ca. 80 and 105 °C (liquid–solid phase transitions).

The solubilities of 3TTN and 2TTN in CH_2Cl_2 are poor, owing to the fact that these substances contain only rigid π-electron-delocalized skeletons. In contrast, C_n-2TTNs possessing four alkyl groups are more soluble in CH_2Cl_2 than 2TTN is. However, the solubility in this solvent decreases as the length of the alkyl chains in C_n-2TTNs increases.

Electrochemical properties[22] of TTNs were evaluated by using cyclic voltammetry and UV–vis absorption spectroscopy. The HOMO energy (E_H) of 3TTN and 2TTN were estimated to be −5.59 and −5.43 eV (Table 3), respectively, based on their respective anodic onset potentials (E_{AO} = +1.23 and +1.07 V vs SCE). This finding indicates that these substances should have a high stability against molecular oxygen.[6b] Indeed, UV–vis absorption spectra of 3TTN and 2TTN remain unchanged when aerated CH_2Cl_2 solutions containing these substances at room temperature stand in the dark for 48 h.[22] The E_H values are nearly the same as those of E'_H obtained by using a quantum chemical calculation [B3LYP/6-31G(d,p)]. The HOMO–LUMO energy gap (ΔE_{H-L}) of 3TTN (3.31 eV), estimated from the absorption edge wavelength ($\lambda_{AB,edge}$), is larger than that of 2TTN (3.26 eV). The difference between ΔE_{H-L} of 3TTN and 2TTN arises from differences in

Table 2. Photoreaction of 2TTE and C_n-2TTEs

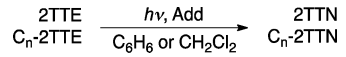

entry	starting material	system	λ_{EX} (nm)	add	time	product	yield (%)
1[a]	2TTE	batch	≥313[b]	I_2	15 h[c]	2TTN	35
2[d]	2TTE	batch	≥313[b]	p-CA	12 h[c]	2TTN	56
3[d]	C_6-2TTE	microflow	365[e]	p-CA	1 min[f,g]	C_6-2TTN	60
4[d]	C_6-2TTE	batch	≥313[b]	p-CA	6 h[c]	C_6-2TTN	40
5[d]	C_8-2TTE	microflow	≥313[h]	p-CA	1 min[f,g]	C_8-2TTN	73
6[d]	C_8-2TTE	batch	≥313[b]	p-CA	3 h[c]	C_8-2TTN	58
7[d]	C_{10}-2TTE	microflow	≥313[h]	p-CA	1 min[f,g]	C_{10}-2TTN	36
8[d]	C_{10}-2TTE	batch	≥313[b]	p-CA	3 h[c]	C_{10}-2TTN	24

[a]In C_6H_6. [b]A 300 W high-pressure mercury lamp with a Pyrex cutoff filter. [c]Irradiation time. [d]In CH_2Cl_2. [e]A 300 mW UV–LED lamp through a quartz glass. [f]Residence time. [g]Flow rate, 0.4 mL min^{-1}. [h]A 80 W medium-pressure mercury lamp with a Pyrex cutoff filter.

DOI: 10.1021/acs.joc.6b00117
J. Org. Chem. 2016, 81, 3168–3176

Table 3. Anodic Onset Potentials (E_{AO}), HOMO Energies (E_H and E'_H), Absorption Edge Wavelengths ($\lambda_{AB,edge}$), HOMO−LUMO Energy Gaps (ΔE_{H-L} and $\Delta E'_{H-L}$), LUMO Energies (E_L and E'_L), and Reorganization Energies (λ_{RE}) of 3TTN, 2TTN, and C_n-2TTNs

compd	solubility (g L^{-1})	E_{AO}[a] (V vs SCE)	E_H[b] (eV)	E'_H[c] (eV)	$\lambda_{AB,edge}$[a] (nm)	ΔE_{H-L}[d] (eV)	$\Delta E'_{H-L}$[c] (eV)	E_L[d] (eV)	E'_L[c] (eV)	λ_{RE}[c] (eV)
3TTN	0.2	+1.23	−5.59	−5.44	375	3.31	4.01	−2.28	−1.43	0.14
2TTN	0.1	+1.07	−5.41	−5.47	390	3.26	4.08	−2.15	−1.39	0.12
C_6-2TTN	10.4	+1.05	−5.39	−5.00	395	3.14	4.13	−2.25	−0.87	0.28
C_8-2TTN	10.4	+1.05	−5.39	−5.00	395	3.14	4.14	−2.25	−0.86	0.31
C_{10}-2TTN	5.3	+1.05	−5.39	−4.92	395	3.14	3.99	−2.25	−0.93	0.29

[a]In CH_2Cl_2. [b]E_H (eV) = $-e[E_{AO}$ (V vs SCE)] − 4.38 (eV). [c]Calculated with (U)B3LYP/6-31G(d,p). [d]ΔE_{H-L} (eV) = $hc/e\lambda_{AB,edge}$. $E_L = E_H + \Delta E_{H-L}$.

their E_H values because their LUMO energy values (E_L = −2.28 and −2.15 eV, respectively) are nearly equal. The E_H, ΔE_{H-L}, and E_L values of C_n-2TTNs are almost the same as that of the parent 2TTN owing to the feeble electron-donating ability of the alkyl groups.

The absorption maxima of 2TTN (297 nm) and 3TTN (286 nm) are derived from respective HOMO → LUMO+1 and HOMO → LUMO+2 electronic transitions [TD-B3LYP/6-311+G(d,p)]. The E_H and E_L of C_n-2TTNs are nearly the same as those of the parent 2TTN because electronic effects exerted by the alkyl groups are negligible. Consequently, the solubilities of C_n-2TTNs are improved without influencing their electronic properties by incorporation of alkyl side chains.

To gain an understanding of the hopping hole-transport process, λ_{RE} related to SET from the neutral species to the corresponding radical cation were calculated by using (U)B3LYP/6-31G(d,p). The results show that λ_{RE} of 3TTN and 2TTN are 0.14 and 0.12 eV, respectively, suggesting that these substances should serve as suitable hole-transporting materials. On the other hand, the λ_{RE} of DNTT and DPh-BTBT are calculated to be 0.12 and 0.23 eV, respectively. Consequently, 3TTN and 2TTN could be promising molecular frameworks for hopping hole transport from the point of view of λ_{RE}. The λ_{RE} values of C_n-2TTNs are higher than that of 2TTN because the electron-donating ability of the alkyl group is overestimated.

X-ray Crystallographic Analysis of 2TTN. X-ray crystallographic analysis of 2TTN (Figure 2)[24] was carried out by using a single-crystal obtained by recrystallization from toluene−*n*-hexane. The analysis shows that 2TTN has a slightly twisted structure in the crystalline state. An S−S contact (d_1 = 3.43 Å) is observed between adjacent 2TTN molecules arranged in an edge-to-edge manner; however, the t_1[18] (B3LYP/6-31G) is calculated to be only 0.1 meV. On the other hand, molecules, having $\pi-\pi$ overlap and a short separation distance (d_2 = 3.41 Å) between the dithienobenzene moieties are arranged in a face-to-face manner. Strong intermolecular $\pi-\pi$ interactions exist in molecular columns of this substance, and t_2 is calculated to be 17.5 meV. van der Waals contacts (d_3 = 2.62 Å and d_4 = 2.57 Å) are present between hydrogen atoms and π-plane in adjacent molecules arranged in an edge-to-face manner. The t_3 and t_4 values, calculated to be 24.3 and 28.4 meV, respectively, are relatively large owing to the existence of CH−π interactions. On the other hand, X-ray crystallographic analyses were not carried out on the derivatives C_n-2TTNs because suitable single crystals could not be generated.

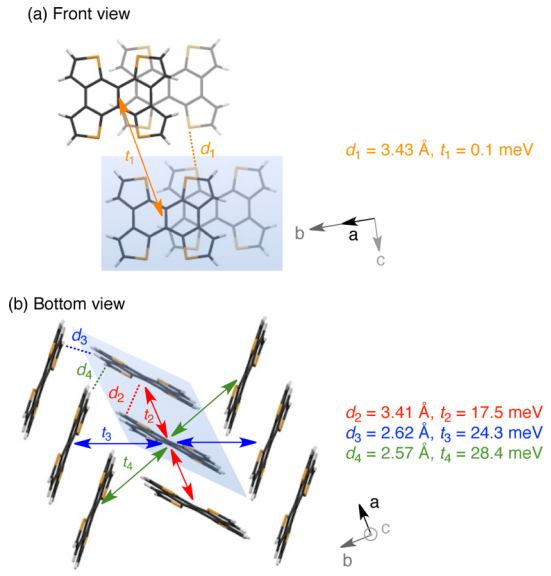

Figure 2. Single-crystal packing structure of 2TTN. Distances (d, dashed line) and transfer integrals (t, double-headed arrow) between neighboring molecules of 2TTN.

Thin-Film Properties of C_n-2TTNs and the Corresponding Solution-Processed OFET Devices. Thin-film properties of C_n-2TTNs were investigated to estimate their solution-processed OFET characteristics. The films were prepared from toluene solutions of C_n-2TTNs (1 wt %) by using spin-coating on glass substrates. The root-mean-square roughness (R_q) of the thin films formed from C_6-, C_8-, and C_{10}-2TTNs are estimated to be 10.5, 8.7, and 18.1 nm (Table 4), respectively, by using atomic force microscopy (AFM) (Figure 3, left). Inspection of polarized microscope images demonstrates that the thin films are polycrystalline (Figure 3, right). Annealing the films at ca. 100 °C causes the formation of multigrain aggregates of C_n-2TTNs on the glass substrate.[22] Note that thin films prepared from chloroform, chlorobenzene, and 1,2-dichlorobenzene solutions of C_n-2TTNs (1 wt %) were found to be inhomogeneous.

On the basis of the results of out-of-plane X-ray diffraction (XRD) measurements (Figure 4a), C_6-2TTN appears to be oriented normal to the glass substrate (edge-on orientation) in the thin film (Figure 5). The out-of-plane d-spacing (d_{out}) for C_6-2TTN of 16.68 Å, obtained from the only XRD peak, is lower than the calculated molecular length [l = 20.36 Å, B3LYP/6-31G(d,p)] of this substance in which all alkyl chains are arranged in a linear manner. C_8- and C_{10}-2TTNs have also orientations in thin films that are similar to that of C_6-2TTN. Furthermore, the results of in-plane XRD measurements (2θ = ca. 23 deg, Figure 4b) show that the d_{in} values increase as the length of the alkyl chains in C_n-2TTNs increases.

To evaluate p-type OFET characteristics of C_n-2TTNs (Figure 6), top-gate bottom-contact devices[25] were fabricated by using the spin-coating method. The OFET devices of C_6-, C_8-, and C_{10}-2TTNs exhibit moderate hole mobilities (μ_{OFET})

DOI: 10.1021/acs.joc.6b00117
J. Org. Chem. 2016, 81, 3168−3176

Table 4. Surface Roughness (R_q), *d*-Spacings (d_{out} and d_{in}), Calculated Molecular Lengths (l), Hole Mobilities of Trial OFET Devices (μ_{OFET}), On/Off Ratios (I_{on}/I_{off}), Subthreshold Swings (SS), and Threshold Voltages (V_{th}) of C_n-2TTNs

compd	R_q (nm)	d_{out} (Å)	d_{in} (Å)	l[a] (Å)	μ_{OFET} ($cm^2\ V^{-1}\ s^{-1}$)	I_{on}/I_{off}	SS (V dec^{-1})	V_{th} (V)
C_6-2TTN	10.5	16.68	3.81	20.36	3.7×10^{-2}	10^6	2.0	−30
C_8-2TTN	8.7	17.33	ND[b]	25.22	1.0×10^{-2}	10^5	2.4	−34
C_{10}-2TTN	18.1	17.33	3.91	30.07	2.4×10^{-3}	10^4	7.9	−31

[a]Obtained by using single-point calculations with B3LYP/6-31G(d,p). [b]Not determined.

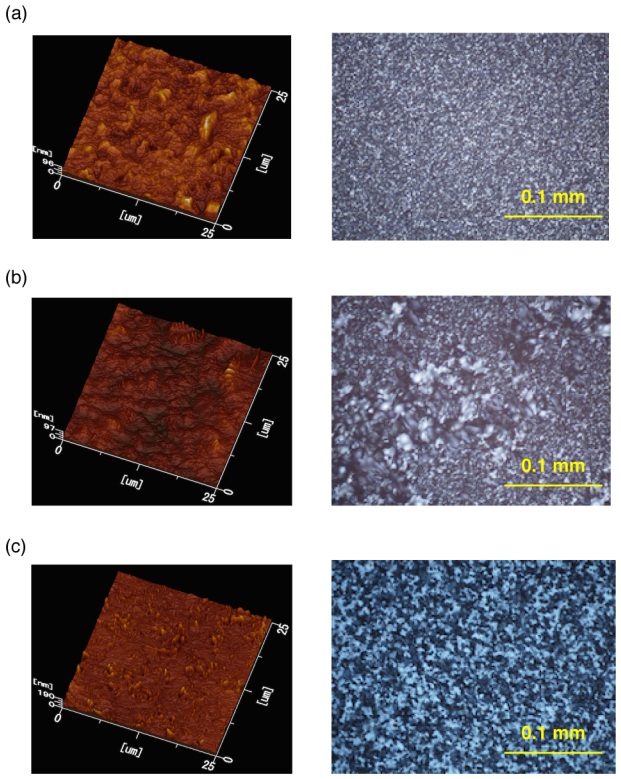

Figure 3. AFM images (left) and polarizing micrographs (right) of spin-coated thin films prepared from toluene solutions of (a) C_6-, (b) C_8-, and (c) C_{10}-2TTNs (1 wt %, respectively) at room temperature.

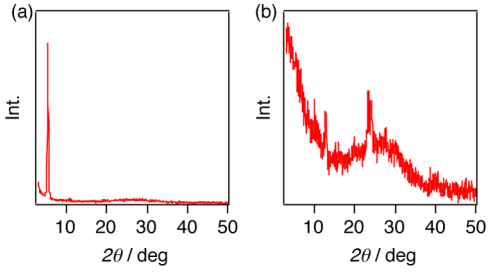

Figure 4. XRD pattern of C_6-2TTN obtained by using (a) out-of-plane and (b) in-plane scans.

of 3.7×10^{-2}, 1.0×10^{-2}, and 2.4×10^{-3} $cm^2\ V^{-1}\ s^{-1}$ in the saturation regions, respectively. Other values including on/off ratios, subthreshold swings, and threshold voltages are also moderate. These results indicate that the OFET properties of C_n-2TTNs become less favorable as the alkyl groups become longer. This phenomenon is a result of an increase in R_q values,[26] a decrease in hole injection efficiency, and extension of the d_{in}-spacing. The observed trend is similar to that seen in inspection of simulated hole mobilities, μ_{am}, of C_n-2TTNs, even

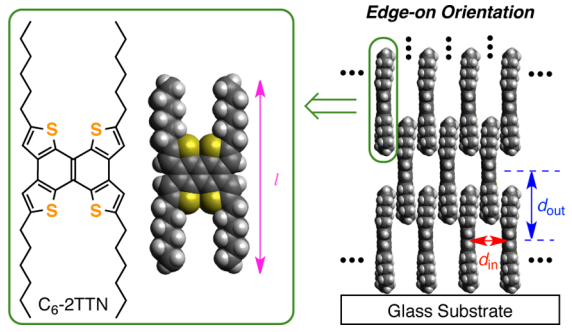

Figure 5. Plausible edge-on orientation model using C_6-2TTN in which all alkyl chains are arranged in a linear manner in the crystalline thin film.

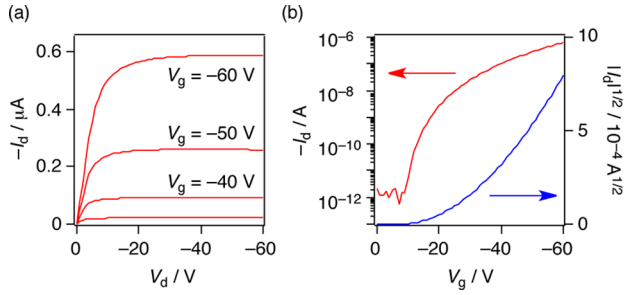

Figure 6. OFET characteristics of C_6-2TTN: (a) output characteristics, and (b) transfer characteristics in the saturation region at a drain voltage of −60 V. Spin-coated thin films were prepared from toluene solutions (1 wt %) at room temperature.

though some differences in structure exist between the actual thin films and the simulated amorphous solids.

CONCLUSION

In the study described above, 2TTN and C_n-2TTNs were developed based on the results of theoretical calculation-inspired investigation. The hole mobility simulations were carried out on amorphous solid structures of 2TTN and C_n-2TTNs. Moderate hole mobilities, μ_{am}, of these compounds were estimated by using an MM-MD simulation on 480 molecules (14000−57600 atoms) and quantum-chemical calculations. The μ_{am} values were found to decrease as the length of alkyl chains increases, a probable result of decreasing *t*. Then C_n-2TTNs were synthesized by using microflow photochemical reactions of C_n-2TTEs with *p*-CA in CH_2Cl_2. 2TTN and C_n-2TTNs appear to have properties that are required for them to serve as hole-transporting materials. Key in this regard is that their HOMO energies are suitable for hole injection and their stabilities in the presence of molecular oxygen are high. The formed polycrystalline film consists of grain and its boundary (i.e., amorphous solid); the latter controls the net mobility. Therefore, it is appropriate to simulate the mobility in the

DOI: 10.1021/acs.joc.6b00117
J. Org. Chem. 2016, 81, 3168−3176

amorphous solid structures. In addition, the simulation of the amorphous solid structure is scientifically more important than that of the single crystal. Fabricated trial top-gate bottom-contact OFET devices constructed using C_n-2TTNs were found to exhibit moderate p-type characteristics. However, as the length of alkyl chains in C_n-2TTNs becomes longer, the μ_{OFET} values tend to become less desirable, a finding that correlates the results arising from theoretical simulations. This behavior might be a consequence of a decrease in hole injection efficiency and an increase in surface roughness and d_{in}-spacing of the spin-coated thin films.

The theoretical simulation method described here appears to be an ideal approach to determining hole mobilities of thin films (macroscopic) based on SET in a pair of molecules (microscopic) in a highly reliable manner. Although the annealing−cooling method was employed for simulated construction of amorphous solid structure, other protocols such as those involving nuclear and surface growth are applicable to these types of systems. An appropriate choice of methods should enable simulation of the characteristics of thin films prepared by vapor deposition and/or solution-casting. Utilization of quantum mechanical and MM-MD simulation methods should become an important tool in the development of OSC materials.

EXPERIMENTAL SECTION

General Methods. Melting points are reported uncorrected. ^{1}H and ^{13}C NMR spectra were recorded at 300 and 75 MHz, respectively. Chemical shifts (δ) are reported in ppm using the signal of tetramethylsilane as an internal standard. Low- and high-resolution (LR- and HR-) fast-atom bombardment (FAB) mass measurements were carried out in a positive mode with 3-nitrobenzyl alcohol (NBA) as the matrix. Mass measurements were also carried out with an LR-atmospheric solid analysis probe (ASAP) method. IR spectra were collected with transmission (KBr pellets) or attenuated total reflection (ATR) methods. Photoreactions using a batch system were carried out by using irradiation from a 300 W high-pressure mercury lamp through a Pyrex cutoff filter. Microflow photoreactions were carried out by using a microflow reactor equipped with a syringe pump, a thermostage, a stainless used steel microchannel (width 1 mm × depth 0.5 mm × length 915 mm), and a 300 mW UV−LED lamp unit with a quartz glass or an 80 W medium-pressure mercury lamp unit with a Pyrex cutoff filter. DSC measurements were carried out on a differential scanning calorimeter. Cyclic voltammetry was performed on an electrochemical analyzer. AFM images were recorded with a scanning probe microscope. XRD measurements were carried out on a high-resolution diffractometer equipped with a Cu Kα radiation source. The OFET electrical characteristics were analyzed using a source meter.

Materials and Solvents. THF and diethyl ether were dried with Nikko Hansen GlassContour solvent-dispensing systems prior to use. For spectroscopic analyses, solvents of spectroscopic grade were used as purchased. For fabrication of OFET devices, acetone and 2-propanol (purity: 99.7% and 99.5%, respectively, Kanto Chemical Co., Inc.) and anhydrous toluene (purity: 99.8%, Sigma-Aldrich Co., Inc.) were used as purchased. Other solvents used for syntheses were purified and dried via the usual methods. Other reagents and solvents were used as purchased unless otherwise noted. Column chromatography was performed with silica gel (neutral, 60N, Merck).

Trial Fabrication of Top-Gate Bottom-Contact OFET Devices and Their Characterizations. The top-gate bottom-contact OFET devices based on C_n-2TTNs were fabricated on a glass substrate under ambient air. Source and drain electrodes (Cr/Au = 3 nm/30 nm) were deposited on the glass substrate by using vacuum evaporation through a metal shadow mask with the channel length (L) of 100 μm and the channel width (w) of 2000 μm. The glass substrates were washed sequentially with acetone and 2-propanol in ultrasonic baths and then cleaned with an UV/O_3 cleaner for 2 h. The toluene solutions of C_n-2TTNs (1 wt %) as semiconductor materials were spin-coated onto the treated glass substrates at room temperature in ambient air to form thin films, which then were dried for 1 h. CYTOP (Asahi Glass CTL-809M, ca. 550 nm on C_6- or C_8-2TTN films, ca. 700 nm on C_{10}-2TTN film) as a gate insulator was similarly spin-coated to create thin films, which then were dried under vacuum at room temperature for 1 h. A gate electrode (Al) was then deposited on the CYTOP. OFET electrical characteristics were measured in an N_2-filled glovebox at room temperature. The field-effect mobility, μ_{OFET}, was calculated using eq 3 in the saturation region

$$I_D = \frac{\mu_{OFET} C_i w}{2L}(V_G - V_{th})^2 \quad (3)$$

where C_i is the capacitance per unit area for the gate insulator, I_D is the drain current, and V_G is the gate voltage.

General Procedures of Preparation of Photoreaction Precursors. The experimental manipulation and physical data of 2DTK are previously reported.[9c] C_6-2DTK was prepared from C_6-2TH,[27a] *n*-BuLi, and *N*,*N*-dimethylcarbamoyl chloride as described below. C_8- and C_{10}-2DTKs were synthesized by using a similar procedure.

Bis(5-n-hexylthien-2-yl) Ketone (C_6-2DTK). To a dry THF (100 mL) solution containing C_6-2TH (5.05 g, 30 mmol) was added dropwise 1.60 M *n*-hexane solution of *n*-BuLi (18.8 mL, 30 mmol) under argon at −78 °C. The mixture was stirred for 1 h. After addition of *N*,*N*-dimethylcarbamoyl chloride (1.38 mL, 15 mmol), the mixture was stirred for 1 h at −78 °C and warmed to room temperature. After being stirred for 15 h, the reaction was quenched with 1 N aq HCl. The resultant mixture was extracted with diethyl ether (30 mL × 3). The combined organic layers were washed with water and brine and dried over anhydrous Na_2SO_4. Concentration of the organic layer under reduced pressure gave residual yellow oil that was subjected to column chromatography [silica gel, *n*-hexane/EtOAc = 10 (v/v)]. The obtained solid was subjected to recrystallization from *n*-hexane−EtOH to give C_6-2DTK (4.90 g, 13.5 mmol, yield 90%) as colorless needles: mp 69−70.5 °C; ^{1}H NMR (300 MHz, $CDCl_3$) δ_{ppm} 0.88 (t, J = 6.8 Hz, 6H), 1.26−1.38 (m, 12H), 1.69 (tt, J = 7.4, 7.4 Hz, 4H), 2.84 (t, J = 7.4 Hz, 4H), 6.85 (d, J = 3.8 Hz, 2H), 7.71 (d, J = 3.8 Hz, 2H); ^{13}C NMR (75 MHz, $CDCl_3$) δ_{ppm} 14.4 (2C), 22.7 (2C), 28.9 (2C), 30.7 (2C), 31.5 (2C), 31.6 (2C), 125.5 (2C), 134.4 (2C), 140.5 (2C), 155.4 (2C), 176.4; IR (KBr) ν/cm^{-1} 1606 (C═O); HR-mass (FAB, NBA) m/z calcd for $[C_{21}H_{30}OS_2]^+$ = 362.1738, found 362.1712.

Bis(5-n-octylthien-2-yl) Ketone (C_8-2DTK). C_8-2DTK was prepared from C_8-2TH[27b] (5.89 g, 30 mmol), 1.60 M *n*-hexane solution of *n*-BuLi (20.1 mL, 32 mmol), and *N*,*N*-dimethylcarbamoyl chloride (1.38 mL, 15 mmol) and purified by using column chromatography [silica gel, *n*-hexane/EtOAc = 20 (v/v)] and recrystallization from EtOH to give pale yellow needles (4.64 g, 11.1 mmol, yield 74%): mp 43−46 °C; ^{1}H NMR (300 MHz, $CDCl_3$) δ_{ppm} 0.88 (t, J = 6.5 Hz, 6H), 1.26−1.38 (m, 20H), 1.72 (tt, J = 7.5, 7.5 Hz, 4H), 2.86 (t, J = 7.5 Hz, 4H), 6.85 (d, J = 3.6 Hz, 2H), 7.71 (d, J = 3.6 Hz, 2H); ^{13}C NMR (75 MHz, $CDCl_3$) δ_{ppm} 14.3 (2C), 22.9 (2C), 29.3 (2C), 29.4 (2C), 29.5 (2C), 30.8 (2C), 31.6 (2C), 32.1 (2C), 125.6 (2C), 133.5 (2C), 140.6 (2C), 155.5 (2C), 178.5; IR (ATR) ν/cm^{-1} 1614 (C═O); HR-mass (FAB, NBA) m/z calcd for $[C_{25}H_{38}OS_2]^+$ = 418.2364, found 418.2360.

Bis(5-n-decylthien-2-yl) Ketone (C_{10}-2DTK). C_{10}-2DTK was prepared from C_{10}-2TH[27b] (8.98 g, 40 mmol), 2.42 M *n*-hexane solution of *n*-BuLi (18.2 mL, 44 mmol), and *N*,*N*-dimethylcarbamoyl chloride (1.84 mL, 20 mmol) and purified by using column chromatography [silica gel, *n*-hexane/EtOAc = 10 (v/v)] and recrystallization from EtOH to give yellow needles (7.55 g, 15.9 mmol, yield 79%): mp 69.5−70.5 °C; ^{1}H NMR (300 MHz, $CDCl_3$) δ_{ppm} 0.88 (t, J = 6.9 Hz, 6H), 1.27−1.34 (m, 28H), 1.69 (tt, J = 7.2, 7.2 Hz, 4H), 2.86 (t, J = 7.2 Hz, 4H), 6.84 (d, J = 3.9 Hz, 2H), 7.71 (d, J = 3.9 Hz, 2H); ^{13}C NMR (75 MHz, $CDCl_3$) δ_{ppm} 14.2 (2C), 22.8 (2C), 29.3 (2C), 29.5 (2C+2C), 29.7 (2C), 29.8 (2C), 30.8 (2C), 31.6 (2C), 32.1 (2C), 125.5 (2C), 133.4 (2C), 140.6 (2C), 155.4 (2C), 178.4;

DOI: 10.1021/acs.joc.6b00117
J. Org. Chem. 2016, 81, 3168−3176

IR (ATR) ν/cm^{-1} 1605 (C═O); HR-mass (FAB, NBA) m/z calcd for $[C_{29}H_{46}OS_2]^+$ = 474.2990, found 474.2967.

2TTE was synthesized by using a McMurry coupling reaction of 2DTK, as described below. C_n-2TTEs were synthesized by using a similar procedure.

Tetra(thien-2-yl)ethene (2TTE). To a dry THF solution (40 mL) at 0 °C under argon was quickly added $TiCl_4$ (0.49 mL, 4.4 mmol). After the solution was stirred for 30 min, activated zinc powder (0.62 g, 9.5 mmol) and pyridine (0.36 mL, 4.5 mmol) were added, and then the mixture was warmed to room temperature. After 2 h of stirring, a THF solution (10 mL) of di(thien-2-yl) ketone (0.77 g, 4.0 mmol) was added. The mixture was stirred for 19 h at 80 °C, quenched with aq Na_2CO_3, and filtered through Celite. The mixture was extracted with EtOAc (50 mL × 1), and the extract was washed with water and brine and dried over anhydrous Na_2SO_4. Concentration of the organic layer under reduced pressure gave a residue that was subjected to column chromatography (silica gel, eluted by $CHCl_3$). The obtained solid was subjected to recrystallization from $CHCl_3$–EtOH to give 2TTE (0.43 g, 1.19 mmol, yield 60%) as orange crystals: mp 196–199 °C; ^{1}H NMR (300 MHz, $CDCl_3$) δ_{ppm} 6.87 (dd, J = 3.6, 1.2 Hz, 4H), 6.95 (dd, J = 5.6, 3.6 Hz, 4H), 7.32 (dd, J = 5.6, 1.2 Hz, 4H); ^{13}C NMR (75 MHz, C_6D_6) δ_{ppm} 126.6 (4C), 126.8 (4C), 130.1 (4C), 130.4 (4C), 144.6 (2C); IR (KBr) ν/cm^{-1} 3120, 3083, 3071, 1793, 1543, 1425, 1349, 1236, 1195, 1129, 1074, 1051, 851, 779, 749, 705, 620; LR-mass (ASAP, relative intensity) m/z 357 ($[M + H]^+$, 31), 81 (C_4HS^+, 100).

Tetrakis(5-n-hexylthien-2-yl)ethene (C_6-2TTE). C_6-2TTE was prepared from bis(5-*n*-hexylthien-2-yl) ketone (1.09 g, 3.0 mmol) and purified by using column chromatography (silica gel, *n*-hexane) and recrystallization from EtOH to give yellow needles (0.70 g, 1.01 mmol, yield 68%): mp 57–58 °C; ^{1}H NMR (300 MHz, $CDCl_3$) δ_{ppm} 0.88 (t, J = 6.6 Hz, 12H), 1.20–1.40 (m, 24H), 1.62 (tt, J = 7.5, 7.5 Hz, 8H), 2.73 (t, J = 7.5 Hz, 8H), 6.59 (d, J = 3.6 Hz, 4H), 6.65 (d, J = 3.6 Hz, 4H); ^{13}C NMR (75 MHz, $CDCl_3$) δ_{ppm} 14.3 (4C), 22.8 (4C), 28.9 (4C), 30.4 (4C), 31.8 (4C + 4C), 123.7 (4C), 127.5 (4C), 129.7 (4C), 142.0 (4C), 148.3 (2C); IR (KBr) ν/cm^{-1} 2959, 2916, 2848, 1459, 1226, 1134, 1028, 806, 782; HR-mass (FAB, NBA) m/z calcd for $[C_{42}H_{60}S_4]^+$ = 692.3578, found 692.3541.

Tetrakis(5-n-octylthien-2-yl)ethene (C_8-2TTE). C_8-2TTE was prepared from bis(5-*n*-octylthien-2-yl) ketone (2.50 g, 6.0 mmol) and purified by using column chromatography (silica gel, *n*-hexane) and recrystallization from $CHCl_3$–EtOH to give a pale yellow powder (1.15 g, 1.43 mmol, yield 48%): mp 67.5–68 °C; ^{1}H NMR (300 MHz, $CDCl_3$) δ_{ppm} 0.88 (t, J = 6.6 Hz, 12H), 1.20–1.40 (m, 40H), 1.62 (tt, J = 7.5, 7.5 Hz, 8H), 2.73 (t, J = 7.5 Hz, 8H), 6.59 (d, J = 3.6 Hz, 4H), 6.65 (d, J = 3.6 Hz, 4H); ^{13}C NMR (75 MHz, $CDCl_3$) δ_{ppm} 14.1 (4C), 22.7 (4C), 29.1 (4C), 29.3 (4C), 29.4 (4C), 30.2 (4C), 31.6 (4C), 31.9 (4C), 123.5 (4C), 126.8 (4C), 129.5 (4C), 141.7 (4C), 148.1 (2C); IR (KBr) ν/cm^{-1} 2953, 2916, 2847, 1764, 1529, 1465, 1254, 1130, 1024, 806, 784; HR-mass (FAB, NBA) m/z calcd for $[C_{50}H_{76}S_4]^+$ = 804.4830, found 804.4871.

Tetrakis(5-n-decylthien-2-yl)ethene (C_{10}-2TTE). C_{10}-2TTE was prepared from bis(5-*n*-decylthien-2-yl) ketone (0.95 g, 2.0 mmol) and purified by using column chromatography [silica gel, *n*-hexane/EtOAc = 5 (v/v)] and recrystallization from $CHCl_3$–EtOH to give a yellow powder (0.42 g, 0.46 mmol, yield 46%): mp 71–73.5 °C; ^{1}H NMR (300 MHz, $CDCl_3$) δ_{ppm} 0.88 (t, J = 6.6 Hz, 12H), 1.20–1.40 (m, 56H), 1.62 (tt, J = 7.5, 7.5 Hz, 8H), 2.73 (t, J = 7.5 Hz, 8H), 6.59 (d, J = 3.6 Hz, 4H), 6.65 (d, J = 3.6 Hz, 4H); ^{13}C NMR (75 MHz, $CDCl_3$) δ_{ppm} 14.3 (4C), 22.9 (4C), 29.3 (4C), 29.6 (4C + 4C), 29.8 (4C), 29.9 (4C), 30.4 (4C), 32.0 (4C), 32.1 (4C), 123.7 (4C), 127.1 (4C), 129.7 (4C), 142.0 (4C), 148.2 (2C); IR (ATR) ν/cm^{-1} 2953, 2916, 2849, 1559, 1465, 1026, 805, 782; HR-mass (FAB, NBA) m/z calcd for $[C_{58}H_{92}S_4]^+$ = 916.6082, found 916.6067. Anal. Calcd for $C_{58}H_{92}S_4$: C, 75.92; H, 10.11; S, 13.98. Found: C, 75.18; H, 9.99.

General Procedure for Photocyclization–Dehydrogenation Reactions. 2TTN was synthesized by using two methods (A and B), as described below. C_n-2TTNs were also synthesized by using two methods (B and C).

Tetrathieno[2,3-a:3′,2′-c:2″,3″-f:3‴,2‴-h]naphthalene (2TTN). Method A (Photoreaction of 2TTE in the Presence of I_2 Using a Batch Reactor). A C_6H_6 (175 mL) solution containing 2TTE (250 mg, 0.70 mmol) and I_2 (360 mg, 1.42 mmol) in a Pyrex test tube was irradiated with a 300 W high-pressure mercury lamp for 15 h at room temperature. After the formed precipitate was separated by filtration, the filtrate was diluted with aq $Na_2S_2O_3$, washed with water and brine, and dried over anhydrous Na_2SO_4. Concentration of the organic layer under reduced pressure gave a residue that was combined with the precipitate and subjected to sublimation (200 °C, 2.6 mmHg) to give 2TTN (87 mg, 0.25 mmol, yield 35%) as a pale yellow powder: mp > 300 °C; ^{1}H NMR (300 MHz, $CDCl_3$) δ_{ppm} 7.89 (d, J = 5.4 Hz, 4H), 8.05 (d, J = 5.4 Hz, 4H); IR (KBr) ν/cm^{-1} 3094, 3078, 1370, 1260, 1084, 884, 724, 641; LR-mass (ASAP, relative intensity) m/z 353 ($[M + H]^+$, 13), 81 (C_4HS^+, 100). ^{13}C NMR spectrum of 2TTN was not able to be obtained due to its poor solubility in $CDCl_3$.

Method B (Photoreaction of 2TTE in the Presence of p-CA Using a Batch Reactor). A CH_2Cl_2 (60 mL) solution containing 2TTE (22 mg, 61 μmol) and *p*-CA (33 mg, 129 μmol) in a Pyrex test tube was irradiated with a high-pressure mercury lamp for 12 h at room temperature. Concentration of the organic layer under reduced pressure gave a residue that was subjected to column chromatography (silica gel, *n*-hexane). The obtained solid was subjected to recrystallization from toluene–*n*-hexane to give 2TTN (12 mg, 0.034 mmol, yield 56%) as colorless needles.

2,5,8,11-Tetra(n-hexyl)tetrathieno[2,3-a:3′,2′-c:2″,3″-f:3‴,2‴-h]-naphthalene (C_6-2TTN) (Method B). C_6-2TTN was prepared by photoirradiation (the high-pressure mercury lamp, 6 h) of a CH_2Cl_2 (100 mL) solution containing C_6-2TTE (364 mg, 0.50 mmol) and *p*-CA (256 mg, 1.0 mmol) and purified by using column chromatography (silica gel, *n*-hexane) and recrystallization from toluene–EtOH to give a pale yellow powder (138 mg, 0.20 mmol, yield 40%): mp 119–122 °C; ^{1}H NMR (300 MHz, $CDCl_3$) δ_{ppm} 0.92 (t, J = 7.2 Hz, 12H), 1.37–1.50 (m, 24H), 1.92 (tt, J = 7.5, 7.5 Hz, 8H), 3.13 (t, J = 7.5 Hz, 8H), 7.60 (s, 4H); ^{13}C NMR (75 MHz, $CDCl_3$) δ_{ppm} 14.1 (4C), 22.6 (4C), 29.0 (4C), 30.9 (4C), 31.6 (4C + 4C), 119.4 (4C), 119.8 (4C), 131.7 (4C), 132.9 (4C), 147.1 (2C); IR (KBr) ν/cm^{-1} 2951, 2927, 2855, 1558, 1462, 1362, 1261, 817, 729; LR-mass (FAB, NBA) m/z 688 (M^+). Anal. Calcd for $C_{42}H_{56}S_4$: C, 73.20; H, 8.19; S, 18.61. Found: C, 73.19; H, 8.33.

Method C (Photoreaction of C_6-2TTE in the Presence of p-CA Using a Microflow Reactor). A CH_2Cl_2 (8 mL) solution containing C_6-2TTE (28 mg, 0.040 mmol) and *p*-CA (20 mg, 0.080 mmol) in a Pyrex gastight syringe was passed through a flow channel in a microflow reactor under irradiation using 300 mW UV–LED lamps through a quartz glass for 1 min (flow rate, 0.4 mL min^{-1}) at room temperature. The reaction mixture was concentrated under reduced pressure, and the obtained residue was subjected to column chromatography (silica gel, *n*-hexane). Recrystallization of the obtained solid from toluene–EtOH gives C_6-2TTN (16 mg, 0.024 mmol, yield 60%) as a pale yellow powder.

2,5,8,11-Tetra(n-octyl)tetrathieno[2,3-a:3′,2′-c:2″,3″-f:3‴,2‴-h]-naphthalene (C_8-2TTN) (Method B). C_8-2TTN was prepared by photoirradiation (high-pressure mercury lamp, 3 h) of a CH_2Cl_2 (100 mL) solution containing C_8-2TTE (162 mg, 0.20 mmol) and *p*-CA (100 mg, 0.40 mmol) and purified by using column chromatography (silica gel, *n*-hexane) and recrystallization from toluene–EtOH to give a pale yellow powder (93 mg, 0.12 mmol, yield 58%): mp 110–112 °C; ^{1}H NMR (300 MHz, $CDCl_3$) δ_{ppm} 0.90 (t, J = 6.6 Hz, 12H), 1.20–1.40 (m, 40H), 1.82 (tt, J = 7.2, 7.2 Hz, 8H), 2.96 (t, J = 7.2 Hz, 8H), 7.51 (s, 4H); ^{13}C NMR (75 MHz, $CDCl_3$) δ_{ppm} 14.3 (4C), 23.1 (4C), 29.7 (4C), 29.8 (4C), 31.2 (4C), 31.8 (4C), 32.0 (4C), 32.3 (4C), 120.1 (4C), 120.7 (4C), 132.6 (4C), 133.8 (4C), 147.2 (2C); IR (KBr) ν/cm^{-1} 2950, 2925, 2853, 1557, 1465, 1362, 1260, 819, 727; LR-mass (FAB, NBA) m/z 800 (M^+). Anal. Calcd for $C_{50}H_{72}S_4$: C, 74.94; H, 9.06; S, 16.01. Found: C, 74.58; H, 9.10.

Method C. C_8-2TTN was also prepared by photoirradiation (a 80 W medium-pressure mercury lamp with a Pyrex cutoff filter, 1 min) to a CH_2Cl_2 (4 mL) solution containing C_8-2TTE (33 mg, 0.041 mmol)

DOI: 10.1021/acs.joc.6b00117
J. Org. Chem. 2016, 81, 3168–3176

and *p*-CA (20 mg, 0.080 mmol) and then purified by using column chromatography (silica gel, *n*-hexane) and recrystallization from toluene−EtOH to give a pale yellow powder (24 mg, 0.030 mmol, yield 73%).

2,5,8,11-Tetra(n-decyl)tetrathieno[2,3-a:3′,2′-c:2″,3″-f:3‴,2‴-h]-naphthalene (C_{10}-2TTN) (Method B). C_{10}-2TTN was prepared by photoirradiation (the high-pressure mercury lamp, 3 h) of a CH_2Cl_2 (50 mL) solution containing C_8-2TTE (184 mg, 0.20 mmol) and *p*-CA (98 mg, 0.40 mmol) and then purified by using column chromatography (silica gel, *n*-hexane) and recrystallization from toluene−EtOH to give pale yellow powder (44 mg, 0.05 mmol, yield 24%): mp 106−107 °C; ^{1}H NMR (300 MHz, $CDCl_3$) δ_{ppm} 0.87 (t, *J* = 6.9 Hz, 12H), 1.22−1.35 (m, 56H), 1.92 (tt, *J* = 7.7, 7.7 Hz, 8H), 3.12 (t, *J* = 7.7 Hz, 8H), 7.60 (s, 4H); ^{13}C NMR (75 MHz, $CDCl_3$) δ_{ppm} 14.3 (4C), 22.9 (4C), 29.5 (4C), 29.6 (4C), 29.7 (4C), 29.8 (4C + 4C), 31.1 (4C), 31.8 (4C), 32.1 (4C), 119.7 (4C), 120.0 (4C), 131.9 (4C), 133.2 (4C), 147.3 (2C); IR (KBr) ν/cm^{-1} 2950, 2925, 2850, 1559, 1465, 1366, 1259, 821; LR-mass (FAB, NBA) *m*/*z* 914 (M^+). Anal. Calcd for $C_{58}H_{88}S_4$: C, 76.25; H, 9.71; S, 14.04. Found: C, 76.07; H, 10.01.

Method C. C_{10}-2TTN was also prepared by photoirradiation (the medium-pressure mercury lamp, 1 min) to a CH_2Cl_2 (6 mL) solution containing C_{10}-2TTE (28 mg, 0.030 mmol) and *p*-CA (15 mg, 0.060 mmol) and then purified by using column chromatography (silica gel, *n*-hexane) and recrystallization from toluene−EtOH to give a pale yellow powder (9 mg, 0.011 mmol, yield 36%).

■ ASSOCIATED CONTENT

Supporting Information

The Supporting Information is available free of charge on the ACS Publications website at DOI: 10.1021/acs.joc.6b00117.

Experimental details, NMR spectra of all new compounds, and (TD-)DFT calculation details (PDF)

X-ray crystallographic data of 2TTN (CIF)

■ AUTHOR INFORMATION

Corresponding Author

*E-mail: ikeda@chem.osakafu-u.ac.jp.

Notes

The authors declare no competing financial interest.

■ ACKNOWLEDGMENTS

A.Y. and Y.M. gratefully acknowledge financial support in the form of the Sasakawa Scientific Research Grant from the Japan Science Society (Nos. 25-304 and 23-307), respectively. T.A. acknowledges financial support in the form of a Grant-in-Aid for the Scientific Research (C) (No. 23550021) and Core Research for Evolutional Science and Technology "High Performance Computing for Multiscale and Multiphysics Phenomena" from the Ministry of Education, Culture, Sport, Science and Technology (MEXT), Japan. E.O. acknowledges financial support in the form of a Grant-in-Aid for Young Scientist (B) (No. 24750044) and the Challenging Exploratory Research (No. 26620034) from the MEXT, Japan. H.N. gratefully acknowledges financial support in the form of a Grant-in-Aid for Scientific Research on Innovative Areas "New Polymeric Materials Based on Element-Blocks" (No. 24102011 in the Area No. 2401) from the MEXT, Japan. H.I. gratefully acknowledges financial support in the form of a Grant-in-Aid for Scientific Research on Innovative Areas "π-Space" (Nos. 21108520 and 23108718 in the Area No. 2007) and "Stimuli-responsive Chemical Species" (No. 24109009), the Scientific Research (B) (Nos. 20044027 and 23350023), and the Challenging Exploratory Research (Nos. 21655016 and 24655037) from the MEXT, Japan.

■ REFERENCES

(1) (a) Hirata, S.; Sakai, Y.; Masui, K.; Tanaka, H.; Lee, S. Y.; Nomura, H.; Nakamura, N.; Yasumatsu, M.; Nakanotani, H.; Zhang, Q.; Shizu, K.; Miyazaki, H.; Adachi, C. *Nat. Mater.* **2014**, *14*, 330−336. (b) Namai, H.; Ikeda, H.; Hoshi, Y.; Kato, N.; Morishita, Y.; Mizuno, K. *J. Am. Chem. Soc.* **2007**, *129*, 9032−9036. (c) Morii, K.; Ishida, M.; Takashima, T.; Shimoda, T.; Wang, Q.; Nazeeruddin, M. K.; Gratzel, M. *Appl. Phys. Lett.* **2006**, *89*, 183510.

(2) (a) Lin, Y.; Li, Y.; Zhan, X. *Chem. Soc. Rev.* **2012**, *41*, 4245−4272. (b) Ooyama, Y.; Uenaka, K.; Sato, T.; Shibayama, N.; Ohshita, J. *RSC Adv.* **2015**, *5*, 2531−2535.

(3) (a) Pron, A.; Gawrys, P.; Zagorska, M.; Djurado, D.; Demadrille, R. *Chem. Soc. Rev.* **2010**, *39*, 2577−2632. (b) Takeya, J.; Yamagishi, M.; Tominari, Y.; Hirahara, R.; Nakazawa, Y.; Nishikawa, T.; Kawase, T.; Shimoda, T.; Ogawa, S. *Appl. Phys. Lett.* **2007**, *90*, 102120.

(4) Cinar, M. E.; Ozturk, T. *Chem. Rev.* **2015**, *115*, 3036−3140.

(5) (a) Anthony, J. E. *Chem. Rev.* **2006**, *106*, 5028−5048. (b) Meng, H.; Sun, F.; Goldfinger, M. B.; Gao, F.; Londono, D. J.; Marshal, W. J.; Blackman, G. S.; Dobbs, K. D.; Keys, D. E. *J. Am. Chem. Soc.* **2006**, *128*, 9304−9305. (c) Merlo, J. A.; Newman, C. R.; Gerlach, C. P.; Kelley, T. W.; Muyres, D. V.; Fritz, S. E.; Toney, M. F.; Frisbie, C. D. *J. Am. Chem. Soc.* **2005**, *127*, 3997−4009. (d) Mori, T.; Nishimura, T.; Yamamoto, T.; Doi, I.; Miyazaki, E.; Osaka, I.; Takimiya, K. *J. Am. Chem. Soc.* **2013**, *135*, 13900−13913. (e) Takimiya, K.; Osaka, I.; Mori, T.; Nakano, M. *Acc. Chem. Res.* **2014**, *47*, 1493−1502. (f) Yamamoto, T.; Takimiya, K. *J. Am. Chem. Soc.* **2007**, *129*, 2224−2225. (g) Mori, H.; Chen, X.-C.; Chang, N.-H.; Hamao, S.; Kubozono, Y.; Nakajima, K.; Nishihara, Y. *J. Org. Chem.* **2014**, *79*, 4973−4983. (h) Takimiya, K.; Ebata, H.; Sakamoto, K.; Izawa, T.; Otsubo, T.; Kunugi, Y. *J. Am. Chem. Soc.* **2006**, *128*, 12604−12605.

(6) (a) Chaudhuri, R.; Hsu, M.-Y.; Li, C.-W.; Wang, C.-I; Chen, C.-J.; Lai, C. K.; Chen, L.-Y.; Liu, S.-H.; Wu, C.-C.; Liu, R.-S. *Org. Lett.* **2008**, *10*, 3053−3056. (b) Wang, X.-Y.; Lin, H.-R.; Lei, T.; Yang, D.-C.; Zhuang, F.-D.; Wang, J.-Y.; Yuan, S.-C.; Pei, J. *Angew. Chem., Int. Ed.* **2013**, *52*, 3117−3120. (c) Brusso, J. L.; Hirst, O. D.; Dadvand, A.; Ganesan, S.; Cicoira, F.; Robertson, C. M.; Oakley, R. T.; Rosei, F.; Perepichka, D. F. *Chem. Mater.* **2008**, *20*, 2484−2494. (d) Wakamiya, A.; Nishimura, H.; Fukushima, T.; Suzuki, F.; Saeki, A.; Seki, S.; Osaka, I.; Sasamori, T.; Murata, M.; Murata, Y.; Kaji, H. *Angew. Chem., Int. Ed.* **2014**, *53*, 5800−5804. (e) Leitch, A. A.; Stobo, K. A.; Hussain, B.; Ghoussoub, M.; Ebrahimi-Takalloo, S.; Servati, P.; Korobkov, I.; Brusso, J. L. *Eur. J. Org. Chem.* **2013**, *2013*, 5854−5863.

(7) Wang, Y.; Zou, S.; Gao, J.; Zhang, H.; Lai, G.; Yang, C.; Xie, H.; Fang, R.; Li, H.; Hu, W. *Chem. Commun.* **2015**, *51*, 11961−11963.

(8) (a) Takimiya, K.; Yamamoto, T.; Ebata, H.; Izawa, T. *Thin Solid Films* **2014**, *554*, 13−18. (b) Wang, X.-Y.; Zhuang, F.-D.; Zhou, X.; Yang, D.-C.; Wang, J.-Y.; Pei, J. *J. Mater. Chem. C* **2014**, *2*, 8152−8161. (c) Wang, J.; Xu, H.; Li, B.; Cao, X.-P.; Zhang, H.-L. *Tetrahedron* **2012**, *68*, 1192−1197. (d) Akkerman, H. B.; Mannsfeld, S. C. B.; Kaushik, A. P.; Verploegen, E.; Burnier, L.; Zoombelt, A. P.; Saathoff, J. D.; Hong, S.; Atahan-Evrenk, S.; Liu, X.; Aspuru-Guzik, A.; Toney, M. F.; Clancy, P.; Bao, Z. *J. Am. Chem. Soc.* **2013**, *135*, 11006−11014. (e) Lei, T.; Wang, J.-Y.; Pei, J. *Chem. Mater.* **2014**, *26*, 594−603. (f) Chang, S.-L.; Lu, C.-W.; Lai, Y.-Y.; Hsu, J.-Y.; Cheng, Y.-J. *Org. Lett.* **2016**, *18*, 368−371.

(9) (a) Mallory, F. B.; Mallory, C. W. *Org. React.* **1984**, *30*, 1−456. (b) Ogaki, T.; Ohta, E.; Yamamoto, A.; Sato, H.; Mizuno, K.; Ikeda, H. *Tetrahedron Lett.* **2014**, *55*, 4269−4273. (c) Yamamoto, A.; Matsui, Y.; Ohta, E.; Ogaki, T.; Sato, H.; Furuyama, T.; Kobayashi, N.; Mizuno, K.; Ikeda, H. *J. Photochem. Photobiol., A* **2015**, DOI: 10.1016/j.jphotochem.2015.10.012. (d) Xiao, S.; Stuart, A. C.; Liu, S.; Zhou, H.; You, W. *Adv. Funct. Mater.* **2010**, *20*, 635−643. (e) Black, H. T.; Liu, S.; Sheares Ashby, V. *Org. Lett.* **2011**, *13*, 6492−6495. (f) Nishide, Y.; Osuga, H.; Iwata, K.; Tanaka, K.; Sakamoto, H. *Bull. Chem. Soc. Jpn.* **2008**, *81*, 1322−1330.

DOI: 10.1021/acs.joc.6b00117
J. Org. Chem. 2016, 81, 3168−3176

(10) Yamamoto, A.; Ohta, E.; Kishigami, N.; Tsukahara, N.; Tomiyori, Y.; Sato, H.; Matsui, Y.; Kano, Y.; Mizuno, K.; Ikeda, H. *Tetrahedron Lett.* **2013**, *54*, 4049−4053.
(11) Fischer, E.; Larsen, J.; Christensen, J. B.; Fourmigué, M.; Madsen, H. G.; Harrit, N. *J. Org. Chem.* **1996**, *61*, 6997−7005.
(12) (a) Dou, C.; Saito, S.; Gao, L.; Matsumoto, N.; Karasawa, T.; Zhang, H.; Fukazawa, A.; Yamaguchi, S. *Org. Lett.* **2013**, *15*, 80−83. (b) Song, J.; Wu, T.; Zhao, X.; Kan, Y.; Wang, H. *Tetrahedron* **2015**, *71*, 1838−1843. (c) Gao, L. *Acta Crystallogr., Sect. C: Cryst. Struct. Commun.* **2013**, *69*, 634−637.
(13) (a) Lefebvre, Q.; Jentsch, M.; Rueping, M. *Beilstein J. Org. Chem.* **2013**, *9*, 1883−1890. (b) Hook, B. D. A.; Dohle, W.; Hirst, P. R.; Pickworth, M.; Berry, M. B.; Booker-Milburn, K. I. *J. Org. Chem.* **2005**, *70*, 7558−7564. (c) Elliott, L. D.; Knowles, J. P.; Koovits, P. J.; Maskill, K. G.; Ralph, M. J.; Lejeune, G.; Edwards, L. J.; Robinson, R. I.; Clemens, I. R.; Cox, B.; Pascoe, D. D.; Koch, G.; Eberle, M.; Berry, M. B.; Booker-Milburn, K. I. *Chem. - Eur. J.* **2014**, *20*, 15226−15232. (d) Mukae, H.; Maeda, H.; Nashihara, S.; Mizuno, K. *Bull. Chem. Soc. Jpn.* **2007**, *80*, 1157−1161. (e) Okamoto, H.; Takane, T.; Gohda, S.; Kubozono, Y.; Sato, K.; Yamaji, M.; Satake, K. *Chem. Lett.* **2014**, *43*, 994−996.
(14) Asada, T.; Ohta, K.; Matsushita, T.; Koseki, S. *Theor. Chem. Acc.* **2011**, *130*, 439−448.
(15) Frisch, M. J.; Trucks, G. W.; Schlegel, H. B.; Scuseria, G. E.; Robb, M. A.; Cheeseman, J. R.; Scalmani, G.; Barone, V.; Mennucci, B.; Petersson, G. A.; Nakatsuji, H.; Caricato, M.; Li, X.; Hratchian, H. P.; Izmaylov, A. F.; Bloino, J.; Zheng, G.; Sonnenberg, J. L.; Hada, M.; Ehara, M.; Toyota, K.; Fukuda, R.; Hasegawa, J.; Ishida, M.; Nakajima, T.; Honda, Y.; Kitao, O.; Nakai, H.; Vreven, T.; Montgomery, J. A., Jr.; Peralta, J. E.; Ogliaro, F.; Bearpark, M.; Heyd, J. J.; Brothers, E.; Kudin, K. N.; Staroverov, V. N.; Kobayashi, R.; Normand, J.; Raghavachari, K.; Rendell, A.; Burant, J. C.; Iyengar, S. S.; Tomasi, J.; Cossi, M.; Rega, N.; Millam, N. J.; Klene, M.; Knox, J. E.; Cross, J. B.; Bakken, V.; Adamo, C.; Jaramillo, J.; Gomperts, R.; Stratmann, R. E.; Yazyev, O.; Austin, A. J.; Cammi, R.; Pomelli, C.; Ochterski, J. W.; Martin, R. L.; Morokuma, K.; Zakrzewski, V. G.; Voth, G. A.; Salvador, P.; Dannenberg, J. J.; Dapprich, S.; Daniels, A. D.; Farkas, Ö.; Foresman, J. B.; Ortiz, J. V.; Cioslowski, J.; Fox, D. J. Gaussian 09, Rev. D.01, Gaussian, Inc., Wallingford, CT, 2009.
(16) Case, D. A.; Darden, T. A.; Cheatham, T. E., III; Simmerling, C. L.; Wang, J.; Duke, R. E.; Luo, R.; Merz, K. M.; Pearlman, D. A.; Crowley, M.; Walker, R. C.; Zhang, W.; Wang, B.; Hayik, S.; Roitberg, A.; Seabra, G.; Wong, K. F.; Paesani, F.; Wu, X.; Brozell, S.; Tsui, V.; Gohlke, H.; Yang, L.; Tan, C.; Mongan, J.; Hornak, V.; Cui, G.; Beroza, P.; Mathews, D. H.; Schafmeister, C.; Ross, W. S.; Kollman, P. A. *AMBER 9*, University of California, San Francisco, 2006.
(17) Marcus, R. A.; Sutin, N. *Biochim. Biophys. Acta, Rev. Bioenerg.* **1985**, *811*, 265−322.
(18) Transfer integrals (t) were calculated by using our hole mobility computational program (Asada, T., Osaka Prefecture University, 2013).
(19) Valeev, E. F.; Coropceanu, V.; da Silva Filho, D. A.; Salman, S.; Bredas, J. L. *J. Am. Chem. Soc.* **2006**, *128*, 9882−9886.
(20) (a) Kuo, M.-Y.; Chen, H.-Y.; Chao, I. *Chem. - Eur. J.* **2007**, *13*, 4750−4758. (b) Ohta, E.; Ogaki, T.; Aoki, T.; Ikeda, H. *Chem. Lett.* **2014**, *43*, 755−757.
(21) Einstein, A. *Ann. Phys.* **1906**, *19*, 371−381.
(22) For details, see the Supporting Information.
(23) Suzuki, T.; Shiohara, H.; Monobe, M.; Sakimura, T.; Tanaka, S.; Yamashita, Y.; Miyashi, T. *Angew. Chem., Int. Ed. Engl.* **1992**, *31*, 455−458.
(24) Crystallographic data (excluding structure factors) for the structures in this paper have been deposited with the Cambridge Crystallographic Data Centre as supplementary publication no. CCDC-1438707 (2TTN).
(25) (a) Takagi, K.; Nagase, T.; Kobayashi, T.; Kushida, T.; Naito, H. *Jpn. J. Appl. Phys.* **2015**, *54*, 011601. (b) Takagi, K.; Nagase, T.; Kobayashi, T.; Naito, H. *Jpn. J. Appl. Phys.* **2014**, *53*, 050305. (c) Takagi, K.; Nagase, T.; Kobayashi, T.; Naito, H. *Org. Electron.* **2014**, *15*, 372−377.
(26) (a) Sirringhaus, H. *Adv. Mater.* **2005**, *17*, 2411−2425. (b) Chua, L. L.; Ho, P. K. H.; Sirringhaus, H.; Friend, R. H. *Adv. Mater.* **2004**, *16*, 1609−1615.
(27) (a) Xia, C.; Fan, X.; Locklin, J.; Advincula, R. C. *Org. Lett.* **2002**, *4*, 2067−2070. (b) Pu, S.; Zhu, S.; Rao, Y.; Liu, G.; Wei, H. *J. Mol. Struct.* **2009**, *921*, 89−100.

DOI: 10.1021/acs.joc.6b00117
J. Org. Chem. 2016, 81, 3168−3176